

Fabrication of a Nanomechanical Mass Sensor Containing a Nanofluidic Channel

Robert A. Barton, B. Ilic, Scott S. Verbridge, Benjamin R. Cipriany, Jeevak M. Parpia, and Harold G. Craighead*

School of Applied and Engineering Physics, Cornell University, Ithaca, New York 14853

ABSTRACT Nanomechanical resonators operating in vacuum are capable of detecting and weighing single biomolecules, but their application to the life sciences has been limited by viscous forces that impede their motion in liquid environments. A promising approach to avoid this problem, encapsulating the fluid within a mechanical resonator surrounded by vacuum, has not yet been tried with resonant sensors of mass less than ~ 100 ng, despite predictions that devices with smaller effective mass will have proportionally finer mass resolution. Here, we fabricate and evaluate the performance of doubly clamped beam resonators that contain filled nanofluidic channels and have masses of less than 100 pg. These nanochannel resonators operate at frequencies on the order of 25 MHz and when filled with fluid have quality factors as high as 800, 2 orders of magnitude higher than that of resonators of comparable size and frequency operating in fluid. Fluid density measurements reveal a mass responsivity of 100 Hz/fg and a noise equivalent mass of 2 fg. Our analysis suggests that realistic improvements in the quality factor and frequency stability of nanochannel resonators would render these devices capable of sensing attogram masses from liquid.

KEYWORDS Nanochannel, nanofluidic, suspended microchannel resonator, nanoelectromechanical systems, mass sensing, dissipation

Micro- and nanomechanical resonators have frequencies of vibration that are sensitive to small amounts of added mass and can therefore be used as inertial microbalances. Since the minimum resolvable mass of a resonant sensor is proportional to its effective mass, progress^{1,2} in miniaturizing these systems has enabled increasingly precise gravimetry; most recently, a carbon nanotube resonator was used to resolve the mass of a single gold atom.³ The extraordinary mass resolution of these devices is well suited to measuring and sensing biological mass, and single cells,⁴ single viruses,⁵ single DNA molecules,⁶ and single proteins⁷ have been detected with this technology. However, in these experiments, the resonator must operate in either vacuum or air to maximize sensitivity. In more biologically relevant liquid media, where viscous drag increases the effective mass and decreases the quality factor of the resonator, achieving equivalent resolution has been a significant challenge. Measurements of bound mass from liquid have been used to monitor important biological interactions in real time;⁸ however, these measurements have resolved hundreds of picograms in contrast to the attogram biological masses that have been resolved by cantilevers operating in vacuum. For resonators operating in liquid, unlike for resonators in air or in vacuum, improving this resolution by miniaturization is difficult because decreasing device size leads to a reduction in Q .⁹ New configura-

tions are therefore necessary to facilitate studies of biological mass under physiological conditions.

Recently, Burg et al. have shown that liquid can be delivered to a resonator without drastically increasing dissipation if that liquid is encapsulated within the resonator instead of surrounding it.¹⁰ In their work, a cantilever with an embedded microfluidic channel known as the suspended microchannel resonator (SMR) was able to resolve the mass of its contents to a single femtogram and was used to determine the mass of single bacterial cells, single nanoparticles, and nanomolar concentrations of proteins. The channel's capabilities as a delivery conduit enabled a new "flow through" mode of measurement, in which the masses of individual analytes were measured as they passed through the cantilever one at a time. Although the SMR has not yet been demonstrated to weigh single viruses or biomolecules because of limited mass resolution, it has been predicted that smaller resonators with embedded fluidic channels will have the required mass resolution because their decreased size will not be accompanied by a drop in quality factor.¹¹ Mass measurements on single viruses, nanoparticles, or biomolecules could provide a useful alternative to dynamic light scattering measurements, which can size particles only in aggregate,¹¹ and other recently demonstrated sizing schemes,¹² in which mass is not measured directly. Despite this promise, and despite work demonstrating the feasibility of fabricating nanochannels inside of nanomechanical resonators,¹³ there has been no demonstrated operation of filled nanofluidic channels inside of resonators with nanoscale cross-sectional dimensions, partly as a consequence of challenging fabrication.¹⁴

* To whom correspondence should be addressed. hgc1@cornell.edu.

Received for review: 01/19/2010

Published on Web: 05/05/2010

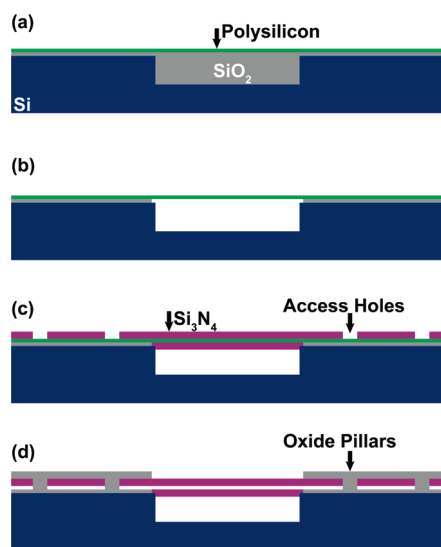


FIGURE 1. Fabrication of nanochannel resonators. A suspended polysilicon doubly clamped beam is conformally coated with stoichiometric nitride to form a polysilicon-filled nanochannel. Next, access holes are etched in the nitride and the polysilicon is removed using XeF₂. Finally, the access holes are filled with oxide to prevent leaks and any oxide deposited on the beam is selectively removed. The vertical scale is exaggerated for clarity.

Here, we report a fabrication technique that is well suited for making suspended nanofluidic channels that hold liquid in vacuum. We produce fluid-filled doubly clamped beams with a mass of ~ 100 pg, 3 orders of magnitude smaller than that of existing fluid-filled resonators,^{11,15,16} and optically actuate and detect their mechanical resonance. These devices, which we refer to as nanochannel resonators, have fundamental resonance frequencies of 25 MHz and quality factors of 500 to 800 when filled with fluid, which is more than 2 orders of magnitude larger than that of resonators of comparable size and frequency operating in liquid.¹⁷ The viscous dissipation mechanisms limiting this quality factor are discussed, and the mass sensitivity of a fluid-filled resonator is calibrated. Our models suggest that realistic improvements in the quality factor and frequency stability of these devices will enable mass sensing from liquid with attogram sensitivity.

The nanochannel resonators presented in this paper were fabricated by coating sacrificial polysilicon doubly clamped beams with low-pressure chemical vapor deposited (LPCVD) stoichiometric silicon nitride. We found that this geometry allowed a XeF₂ gas etchant to hollow out suspended doubly clamped beams up to 20 μm long. The details of this process are presented in Figure 1. We began by etching trenches approximately 2 μm deep in a standard 500 μm thick silicon wafer using an inductively coupled plasma etch process. The trenches were subsequently overfilled with approximately 2.3 μm of plasma-enhanced chemical vapor deposited (PECVD) SiO₂. The oxide was flattened by chemical mechanical polishing, leaving oxide-filled trenches in the plane of the silicon wafer. The wafers were then coated by 140

nm of PECVD oxide followed by 107 nm of LPCVD polysilicon, yielding the structure shown in Figure 1a.

Next, the sacrificial polysilicon layer was patterned to form the structure of the on-chip fluidics. Doubly clamped polysilicon beams up to 20 μm long and ranging in width from 650 nm to 2.5 μm were patterned across the oxide-filled trenches using standard photolithography followed by reactive ion etching (RIE) in CF₄. On either side of the doubly clamped beams, fluid delivery channels 20 μm wide and approximately 6 mm long were defined in polysilicon to allow transportation of fluid to the narrow doubly clamped beams. The sacrificial doubly clamped beams were suspended using buffered oxide etch (BOE 6:1), rinsed in water, and nitrogen dried, resulting in the geometry shown in Figure 1b. Next, an LPCVD technique described in detail elsewhere¹⁸ was used to deposit 337 nm of stoichiometric silicon nitride with an inherent tensile stress of 1200 MPa.¹⁹ The silicon nitride conformally coated the suspended doubly clamped beams to form a polysilicon-filled nanochannel. As shown in Figure 1c, circular access holes 2 μm in diameter were patterned every 10 μm along the entire length of the silicon nitride fluid delivery channel by photolithography and RIE in CF₄. Before removing the resist defining the access holes, the sacrificial polysilicon was removed using a XeF₂ gas etchant. Finally, the resist was removed and a PECVD layer of oxide was used to seal the access holes. The oxide was allowed to cover the entire chip and was then selectively removed from the suspended beam and the outer edges of the fluid delivery channels with photolithography and BOE. The resulting devices are shown in Figure 1d and in Figure 2. NanoPorts (Upchurch Scientific, Oak Harbor, WA) were affixed to the wafer above the open portions of the fluid delivery channels to serve as fluid reservoirs (see Figure 2c).

Before the suspended channels were filled with liquid, their resonance was actuated and detected using an optical approach described in detail elsewhere.²⁰ Briefly, a 405 nm amplitude-modulated diode laser (Picoquant, Berlin, Germany) injects thermal energy into the system at a given frequency and excites motion through thermal expansion and contraction of the device layer. The resonator motion is monitored with a red (633 nm) continuous wave HeNe laser focused on the device. The device and the underlying silicon substrate form a Fabry–Perot interferometer that transduces device motion into oscillations in the reflected red light intensity; these variations are monitored with a fast photodiode connected to a spectrum analyzer. We note that for all of the fluids studied here, the estimated change in temperature resulting from their absorbed laser power is negligible (less than 0.01 K) owing to their small optical absorbance at these wavelengths.²¹ Furthermore, we operate in a regime of laser power in which the measured resonant frequencies are independent of power to within experimental error. In order to eliminate the dissipative effects of air, the chip with attached NanoPorts was placed in a vacuum chamber for resonance measurements. All

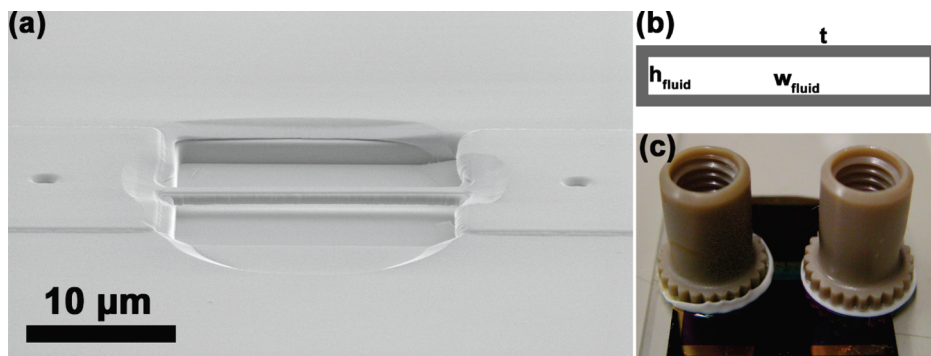


FIGURE 2. (a) Scanning electron microscope image of a suspended nanofluidic channel $20\ \mu\text{m}$ in length. The channel has been hollowed out by a gas etch that enters through circular holes on either side of the channel. These holes have been filled with oxide to prevent leakage, leaving visible impressions. (b) Schematic cross section of a nanochannel resonator. The hollow fluidic channels have inner height $h_{\text{fluid}} = 107\ \text{nm}$ and inner widths w_{fluid} ranging from $650\ \text{nm}$ to $2.5\ \mu\text{m}$. The channels are surrounded by a conformal coating of Si_3N_4 with thickness $t = 337\ \text{nm}$. (c) NanoPorts are attached to the chip above the outer edges of the fluid delivery channels to act as fluid reservoirs and to enable filling of the channels.

experiments were conducted at pressures below 1 Torr, where viscous damping from air is negligible (see Supporting Information).

After interrogating unfilled resonators, we filled the resonators with liquid and characterized their performance in the filled state. We wetted the nanofluidic channels by pipetting a 70% ethanol, 30% H_2O solution into one of the reservoirs and allowing the channels to fill by capillary action. The progress of the fluid along the length of the channel could be monitored with an optical microscope because of the significant difference between the refractive index of air and that of the liquid. Typically, the suspended channels filled in a matter of minutes by capillary forces. We then capped the NanoPorts and returned the chip to the vacuum chamber for resonance measurements.

The results of the optical resonance measurements before and after filling are shown in Figure 3. Before filling, fundamental resonances of the $20\ \mu\text{m}$ long nanochannel resonators were on the order of 25 MHz, and quality factors ranged from 1300 to 7000. After filling, the resonance frequency and quality factor dropped for all of the four devices studied. Figure 3 shows the quality factor of one device before ($Q \sim 2900$) and after ($Q \sim 760$) filling with the ethanol solution. A resonator on the same chip that was unfilled maintained a quality factor of ~ 4000 , confirming that the quality factor decrease in the filled channels was a result of the introduction of fluid.

To calibrate the mass responsivity of nanochannel resonators, we filled the NanoPorts with a series of liquids of varying densities, allowing each liquid to diffuse into the channels. In addition to the ethanol solution, we introduced H_2O and D_2O solutions containing 0.5% Triton X-100 as a surfactant. The results for one of the channels studied are shown in Figure 4. Standard theory for a beam uniform along its length predicts that the fractional change in resonance frequency caused by a mass loading per unit length of Δm_A is given by $\Delta f/f = -1/2 (\Delta m_A/m_A)$, where m_A is the

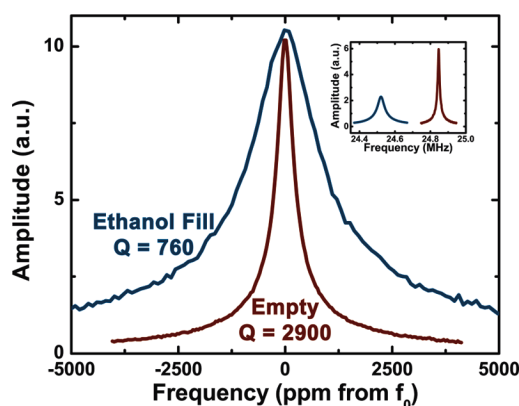


FIGURE 3. Quality factor of a resonant nanochannel (channel width = $1.85\ \mu\text{m}$) before and after filling. The resonance peaks have been overlaid and normalized in amplitude to emphasize the difference in width. Inset: the same peaks are shown in frequency space to display the frequency shift caused by the addition of liquid to the device.

mass per unit length of the bare resonator.¹⁶ Since $\Delta m_A = \Delta \rho_{\text{fluid}} A_{\text{fluid}}$, where $\Delta \rho_{\text{fluid}}$ is the change in fluid density and A_{fluid} is the cross-sectional area of the channel, we expect the change in resonance frequency to be proportional to the density of the fluid. Figure 4b shows a linear dependence of the measured frequency as a function of density in agreement with these theoretical predictions. The device responsivity can be obtained from the slope of the linear fit, which is $\Delta f/\Delta \rho = -406 \pm 8\ \text{kHz}/(\text{g cm}^{-3})$. The magnitude of this response is within 12% of that expected from the above theory in a uniform resonator of the defined dimensions. The difference is within fabrication tolerances. All devices studied showed decreasing frequency with increasing density and linear fits yielded slopes similar to the value quoted above. For some devices, the data showed more scatter around the linear dependence of frequency on density. We attribute these deviations to shifting debris that may have

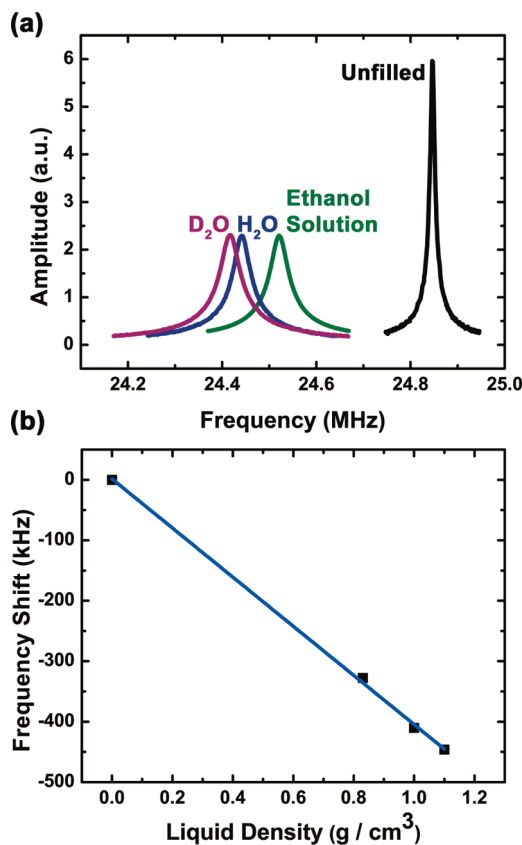


FIGURE 4. The sensitivity of a resonant nanochannel to mass loading was calibrated using liquids of different densities. (a) From right to left, the channel is unfilled, filled with an ethanol solution, filled with H₂O, and filled with D₂O. (b) The center frequency of each peak from (a) is plotted as a function of the liquid density. The slope of the linear fit is $\Delta f/\Delta\rho = -406 \pm 8$ kHz/(g cm⁻³). Error bars representing 1 standard deviation are smaller than the black squares.

entered the channels through the reservoirs or to contamination of the outside of the device over time.

It is important to understand the behavior of both the frequency and quality factor of the fluid-filled nanochannels in order to evaluate the usefulness of the devices. We model these devices as doubly clamped beams under tension, for which the expected resonant frequency is²²

$$f = \frac{\pi(2n+1)^2}{8L^2} \sqrt{\frac{EI}{\rho A}} \sqrt{1 + \frac{0.97}{(n+1)^2} \frac{\sigma AL^2}{EI}} \quad (1)$$

where E is Young's modulus, I is the second moment of area, ρ is the density of the resonator body, A is the cross-sectional area of the nitride material, σ is the stress, L is the length of the device, and $n = 1, 2, \dots$, is the mode number. If we use the targeted dimensions of the device studied in Figure 3 and previously measured values for the nitride material, $E = 211$ GPa, $\rho = 2700$ kg/m³, and $\sigma = 1200$ MPa,¹⁹ we find that the expected fundamental frequency is 26.2 MHz. If we consider the slow but finite rate at which XeF₂ etches nitride,

we find that the sidewalls and undersides of the channels should be approximately 70 nm thinner than the top sides, which were protected by resist during the XeF₂ etch. Taking this asymmetry into account and using scanning electron microscopy to obtain a precise value for beam length, we find that the expected fundamental frequency of the device studied in Figure 3 is 24.8 MHz, which is in good agreement with our observations. We note that for these parameters, the first and second terms under the square root (the bending and tension contributions to the resonant frequency, respectively) contribute almost equally to the frequency.

Equation 1 also predicts the frequencies of higher order modes that we were able to measure with the optical technique used here. For example, measurements showed that the water-filled device studied in Figure 4 had an $n = 2$ mode with $f = 59$ MHz and $Q = 460$ and an $n = 3$ mode with $f = 105$ MHz and $Q = 411$ (see Supporting Information). These frequencies agree well with the above theory. One can imagine a number of interesting sensing applications for resonators operating in these higher order modes, in which flowing analytes will pass both nodes and mass-sensitive regions as they traverse a single channel. For instance, accurate measurements of analyte velocity could be obtained by measuring the time between dips in frequency as a single particle traverses the channel, or concomitant dips in frequency could be used to differentiate real signals from false positives. The increasing fQ product for higher order modes also points to the possibility of enhancing mass resolution by monitoring higher-order modes.

One of our most striking results is the dramatic reduction in quality factor caused by the introduction of liquid to the resonant nanochannel. In previous studies of suspended microchannel resonators,¹⁰ water could be added to the channel without reducing quality factor, while for the device in Figure 3 the addition of liquid decreases the quality factor by a factor of 4. This result is surprising considering that the dominant mode of dissipation in the SMR is a shearing of the bulk fluid that is free to move independently of the channel walls. This effect should be comparatively weak in our devices because the small channel height ensures that the fluid tracks the resonator motion throughout the channel. More quantitatively, the viscous penetration depth for a surface resonating at frequency ω in a fluid of dynamic viscosity ν is²³ $\delta = (2\nu/\omega)^{1/2}$, and the magnitude of the shearing effect varies with the dimensionless frequency $\beta = 2h_{\text{fluid}}^2/\delta^2$, where h_{fluid} is the channel height.¹¹ For the resonant nanochannels presented here, $\delta \sim 100$ nm and $h_{\text{fluid}} = 107$ nm, so that $\beta \approx 2$. As a function of β , Burg et al.^{11,24} model the shear loss in a cantilever of length L , thickness h_{cant} , and width b_{cant} containing a fluidic channel of width b_{fluid} and height h_{fluid} as

$$Q_{\text{shear}} \approx \left(0.152\sqrt{\beta} + \frac{38.7}{\beta}\right) \left(\frac{\rho_{\text{cant}}}{\rho_{\text{fluid}}}\right) \left(\frac{h_{\text{cant}}}{h_{\text{fluid}}}\right) \left(\frac{b_{\text{cant}}}{b_{\text{fluid}}}\right) \left(\frac{L}{h_{\text{fluid}}}\right)^2 \quad (2)$$

If, to obtain a rough estimate, we assume that our device is a cantilever with $L = 10 \mu\text{m}$, $h_{\text{cant}} = 781 \text{ nm}$, $b_{\text{cant}} = 2.5 \mu\text{m}$, $h_{\text{fluid}} = 107 \text{ nm}$, $b_{\text{fluid}} = 1.85 \mu\text{m}$, $\rho_{\text{cant}} = 2700 \text{ kg/m}^3$, and $\rho_{\text{fluid}} = 1000 \text{ kg/m}^3$, we find that the shear-limited quality factor of the resonators presented here is $Q_{\text{shear}} \sim 5 \times 10^6$. Thus, we ignore the contribution of fluid shear to our device. Indeed, when the SMR was operated in the regime of $\beta \approx 2$, as was achieved by filling the device with a liquid of high viscosity, it was found that the quality factor was limited by pumping of fluid in and out of the channel resulting from the off-axis placement of the fluidic channel. The analogous effect for doubly clamped beams may be important in the nanochannel resonators studied here, as we now explore.

If a nanochannel is situated with an offset from the neutral axis of one of the doubly clamped beams described here, then the lengths of different parts of the channel will increase or decrease as the beam bends, altering the local volumes of the channel and effectively pumping fluid back and forth within the beam. During resonance, the energy required to move the channel against the fluid will contribute to the dissipation. At the low Reynolds numbers under consideration, the work required to push the fluid through the channel is governed by viscosity and can be derived from the standard equation for planar Poiseuille flow,²⁵ $P = (12\eta L/h_{\text{fluid}}^2)v$, where v is the fluid velocity, η is the viscosity, and P is the pressure required to propel the fluid. To simplify the calculation, we assume an incompressible fluid in a doubly clamped beam with no tension, in which case the total volume of the off-axis channel is conserved and fluid moves only within the beam. Using this model, we find that the quality factor expected for a fluidic channel a distance y away from the neutral axis is

$$Q_{\text{pumping}} \approx \frac{1}{148} \left(\frac{\omega}{\eta}\right) \left(\frac{h_{\text{beam}} b_{\text{beam}} \rho_{\text{beam}} L^2}{y^2}\right) \left(\frac{h_{\text{fluid}}}{w_{\text{fluid}}}\right) \quad (3)$$

where h_{beam} , b_{beam} , and ρ_{beam} are the outer height, outer width, and density of the nitride structure, respectively. For our channel, we expect an off-axis placement of $y \approx 35 \text{ nm}$ as a result of the asymmetric etching of nitride by XeF_2 as described earlier. In this case, eq 3 predicts a pumping-limited quality factor of $Q_{\text{pumping}} \sim 88000$ for a nanochannel filled with ethanol. This is nearly 2 orders of magnitude different from the fluid-limited quality factor of $Q_{\text{fluid}} = 1100$ suggested by Figure 3. It is important to emphasize that eq 3 assumes an infinitely thin channel in a doubly clamped beam with no tension, while our device has significant tension and therefore undergoes stretching in its resonance.

When stretching occurs, the volume of the channel is not conserved, and the dissipation from pumping includes the work required to pump fluid into the delivery channels. However, the contribution of the off-axis channel placement to stretching is small, and we estimate $Q \sim 10^7$ from this effect using a calculated mode shape.²² Other stretching effects may be important, and further work is required to understand the dominant dissipation mechanism in these devices. We note that while the off-axis incompressible fluid pumping effect that limited the Q in¹¹ appears unimportant in the resonators described here, the channel asymmetry could be further reduced by making the XeF_2 etch step isotropic, so that the fluidic channel remains in the center of the resonator. The fabrication technique presented here is in fact ideally suited to making fluidic channels that are precisely centered on the neutral axis of the resonator, as is necessary for optimizing the performance of devices at this scale.

Ultimately, the sensing capability of nanochannel resonators will depend on their response to absolute mass. If we divide the slope of the linear fit in Figure 4b by the expected volume of the channel, we find that the response of the channel to absolute mass is $\Delta f/\Delta m = -103 \pm 2 \text{ Hz/fg}$. This response must be balanced against the precision with which we can detect the frequency of the resonator. Using the optical resonance techniques described to repeatedly measure the device response to a swept frequency and fitting the response in real time to identify the peak, we find that the short-term frequency noise in our measurements is typically 200 Hz peak to peak in a 250 mHz bandwidth. Therefore, the minimum fluid mass resolvable by a resonant nanochannel in the current configuration is about 2 fg. Over long time periods (on the order of minutes), the precision with which the frequency can be resolved is limited by drift. However, we expect the mass resolution to be dominated by short-term frequency stability in flow-through mode, in which mass is measured on smaller time scales as an analyte passes through the device. Currently, the frequency stability is on the order of 1 % of the peak width, which is comparable to previous measurements utilizing optical drive and detection techniques.⁶ It might be possible to reduce frequency noise by improving the signal-to-noise ratio of the resonance frequency measurements, which is currently 100–400. Additionally, if the channel walls are narrowed and the quality factor of filled resonators can be raised to that of unfilled resonators, then the sensitivity will be improved by an order of magnitude. Finally, the frequency stability of the device could be improved by implementing temperature control.¹⁰ If the noise floor of the device is improved to the thermoelastic limit, it should be possible to detect masses on the order of 100 zg (1 zg = 10^{-21} g) in a 10 Hz bandwidth.²⁶

Our results demonstrate that conformally coating a sacrificial doubly clamped beam with a silicon nitride structural material is a feasible way to fabricate a fluid-filled resonator

with a mass of less than 100 pg. By operating fluid-filled resonators in vacuum, we are able to measure the contribution of fluid to the quality factor of these resonators. Like their microscale counterparts, nanoscale resonators filled with fluid show a significant improvement in quality factor compared with solid resonators of similar dimensions and frequency in liquid. However, it is clear that the dissipation in nanochannel resonators is still dominated by fluid. Further work is required to understand the physics of this phenomenon.

We anticipate that the large body of experimental techniques that have been developed for nanofluidics will find a natural application to nanochannel resonators. For instance, electrophoresis can be used to efficiently drive analytes through a resonant nanochannel for mass sensing in flow-through mode. We envision that this application will be useful in measuring the masses of quantum dots and biomolecular analytes for which single molecule resolution is important, such as amyloid beta.¹¹ Though improved frequency resolution will be necessary for these applications, this demonstration of the performance of low-mass fluid-filled resonators is an important step toward the goal of sensing mass from fluid at the single biomolecule scale.

Acknowledgment. The authors thank S. Krylov, J. D. Cross, and P. S. Waggoner for useful technical discussions. Fabrication was performed at the Cornell NanoScale Facility, a member of the National Nanotechnology Infrastructure Network, which is supported by the National Science Foundation (Grant ECS-0335765). This work was supported by the Cornell Center for Materials Research (CCMR) with funding from the Materials Research Science and Engineering Center Program of the National Science Foundation (cooperative agreement DMR 0520404), and by the Defense Advanced Research Projects Agency (DARPA) under HR0011-06-1-0042.

Supporting Information Available. Figures showing the dependence of the quality factor of a nanochannel resonator on pressure and three resonant modes of a single fluid-filled nanochannel resonator. This material is available free of charge via the Internet at <http://pubs.acs.org>.

REFERENCES AND NOTES

- (1) Ilic, B.; Craighead, H. G.; Krylov, S.; Senaratne, W.; Ober, C.; Neuzil, P. *J. Appl. Phys.* **2004**, *95* (7), 3694–3703.
- (2) Yang, Y. T.; Callegari, C.; Feng, X. L.; Ekinici, K. L.; Roukes, M. L. *Nano Lett.* **2006**, *6* (4), 583–586.
- (3) Jensen, K.; Kim, K.; Zettl, A. *Nat. Nanotechnol.* **2008**, *3* (9), 533–537.
- (4) Ilic, B.; Czaplowski, D.; Zalalutdinov, M.; Craighead, H. G.; Neuzil, P.; Campagnolo, C.; Batt, C. *J. Vac. Sci. Technol., B* **2001**, *19* (6), 2825–2828.
- (5) Gupta, A.; Akin, D.; Bashir, R. *Appl. Phys. Lett.* **2004**, *84* (11), 1976–1978.
- (6) Ilic, B.; Yang, Y.; Aubin, K.; Reichenbach, R.; Krylov, S.; Craighead, H. G. *Nano Lett.* **2005**, *5* (5), 925–929.
- (7) Naik, A. K.; Hanay, M. S.; Hiebert, W. K.; Feng, X. L.; Roukes, M. L. *Nat. Nanotechnol.* **2009**, *4* (7), 445–450.
- (8) Braun, T.; Ghatkesar, M. K.; Backmann, N.; Grange, W.; Boulanger, P.; Letellier, L.; Lang, H. P.; Bietsch, A.; Gerber, C.; Hegner, M. *Nat. Nanotechnol.* **2009**, *4* (3), 179–185.
- (9) Sader, J. E. *J. Appl. Phys.* **1998**, *84* (1), 64–76.
- (10) Burg, T. P.; Godin, M.; Knudsen, S. M.; Shen, W.; Carlson, G.; Foster, J. S.; Babcock, K.; Manalis, S. R. *Nature* **2007**, *446* (7139), 1066–1069.
- (11) Burg, T. P.; Sader, J. E.; Manalis, S. R. *Phys. Rev. Lett.* **2009**, *102*, (22).
- (12) Zhu, J.; Ozdemir, S. K.; Xiao, Y.; Li, L.; He, L.; Chen, D.; Yang, L. *Nat. Photonics* **2010**, *4*, 46–49.
- (13) Verbridge, S. S.; Edel, J. B.; Stavits, S. M.; Moran-Mirabal, J. M.; Allen, S. D.; Coates, G.; Craighead, H. G. *J. Appl. Phys.* **2005**, *97*, (12).
- (14) Eom, K.; Yang, J.; Park, J.; Yoon, G.; Sohn, Y. S.; Park, S.; Yoon, D. S.; Na, S.; Kwon, T. *Int. J. Mol. Sci.* **2009**, *10* (9), 4009–4032.
- (15) Burg, T. P.; Manalis, S. R. *Appl. Phys. Lett.* **2003**, *83* (13), 2698–2700.
- (16) Burg, T. P.; Mirza, A. R.; Milovic, N.; Tsau, C. H.; Popescu, G. A.; Foster, J. S.; Manalis, S. R. *J. Microelectromech. Syst.* **2006**, *15* (6), 1466–1476.
- (17) Verbridge, S. S.; Bellan, L. M.; Parpia, J. M.; Craighead, H. G. *Nano Lett.* **2006**, *6* (9), 2109–2114.
- (18) Southworth, D. R.; Barton, R. A.; Verbridge, S. S.; Ilic, B.; Fefferman, A. D.; Craighead, H. G.; Parpia, J. M. *Phys. Rev. Lett.* **2009**, *102*, (22).
- (19) Verbridge, S. S.; Parpia, J. M.; Reichenbach, R. B.; Bellan, L. M.; Craighead, H. G. *J. Appl. Phys.* **2006**, *99* (12), 8.
- (20) Ilic, B.; Krylov, S.; Aubin, K.; Reichenbach, R.; Craighead, H. G. *Appl. Phys. Lett.* **2005**, *86*, (19).
- (21) Stone, J. *J. Opt. Soc. Am.* **1972**, *62* (3), 327–333.
- (22) Bokaian, A. *J. Sound Vib.* **1990**, *142* (3), 481–498.
- (23) Landau, L.; Lifshitz, E. *Fluid Mechanics*; Pergamon: London, 1959.
- (24) Sader, J. E.; Burg, T. P.; Manalis, S. R. *J. Fluid. Mech.* **2010**, *650*, 215–250.
- (25) Munson, B.; Young, D. F.; Okiishi, T. H. *Fundamentals of Fluid Mechanics*; John Wiley & Sons, Inc.: New York, 1998.
- (26) Ekinici, K. L.; Yang, Y. T.; Roukes, M. L. *J. Appl. Phys.* **2004**, *95* (5), 2682–2689.